International Journal of Impact Engineering 50 (2012) 76–82

Contents lists available at SciVerse ScienceDirect

International Journal of Impact Engineering

journal homepage: www.elsevier.com/locate/ijimpeng

Optical techniques for measuring the shock Hugoniot using ballistic projectile and high-explosive shock initiation

F.R. Svingala [a,*], M.J. Hargather [b], G.S. Settles [a]

[a] The Pennsylvania State University, Gas Dynamics Lab, Department of Mechanical and Nuclear Engineering, 301D Reber Building, University Park, PA 16802, USA
[b] New Mexico Institute of Mining and Technology, Department of Mechanical Engineering, Brown Hall 14, Socorro, NM 87801, USA

ARTICLE INFO

Article history:
Received 15 May 2012
Received in revised form
29 July 2012
Accepted 1 August 2012
Available online 31 August 2012

Keywords:
Shock hugoniot
Shadowgraphy
Polyurea
Polyurethane
High-speed videography

ABSTRACT

The shock Hugoniot is a fundamental relationship between pressure, volume, and energy for a given medium. Accurate knowledge of the Hugoniot for a material is critical in order to determine its response to shock waves and high-velocity impacts. Traditionally, the shock Hugoniot is measured on a point-by-point basis by a series of high-velocity impact experiments. Observations are typically confined to pointwise pressure or velocity measurements at the free-surfaces of the sample. In this work, shock waves are initiated in transparent polyurethane and semi-opaque polyurea samples using exploding bridgewires, aluminum ballistic projectiles, and gram-scale explosive charges. Shock waves and material motion are observed optically by shadowgraphy using a high-speed-digital camera recording at up to 10^6 frames/s. Ballistic impact, producing a constant-strength shock wave, is combined with these optical techniques to obtain a single shock Hugoniot point per test. A gram-scale explosive charge produces a shock wave in the material sample that is initially strong, but attenuates to near the bulk sound speed as it transits the polymer sample. With optical access to the entire sample, multiple shock and particle velocity combinations may be observed in a single test, allowing the measurement of a shock Hugoniot curve in fewer experiments than by traditional methods. These techniques produce data in general agreement with an extrapolation of published Hugoniot data for polyurethane and polyurea.

© 2012 Elsevier Ltd. All rights reserved.

1. Introduction

Shock waves are sharp discontinuities in pressure, density, and internal energy in any continuous material. They can result from a localized rapid release of energy, as in an explosion, or from high-velocity impacts. The behavior of a material under shock loading is defined by the Rankine–Hugoniot equations, which represent conservation of mass, momentum, and energy across a shock wave. These equations define a locus of possible pressure-density-energy states that a material may attain across a shock wave. The steady-state form of these relations are given in equations (1)–(3)

$$\frac{\rho_2}{\rho_1} = \frac{U_s - U_{p1}}{U_s - U_{p2}} \tag{1}$$

$$P_2 - P_1 = \rho_1 (U_{p2} - U_{p1})(U_s - U_{p1}) \tag{2}$$

$$e_2 - e_1 = \frac{1}{\rho_1}\frac{(P_2 U_{p2} - P_1 U_{p1})}{(U_s - U_{p1})} - \frac{1}{2}\left(U_{p2}^2 - U_{p1}^2\right) \tag{3}$$

where, ρ represents density, U_s represents shock wave velocity, U_p represents the velocity of the material through which the shock passes, and e represents internal energy. Variables with a subscript of 1 represent values in the unshocked material while 2 represents the shocked values (Fig. 1).

Knowledge of material shock behavior is critical for the design of systems which may be subjected to explosive or projectile loading, e.g., infantry helmets, ship hulls, building facades, etc. Recently, there has been a push to develop systems to protect people and equipment from relatively low-pressure shock waves, i.e., those with overpressures in the kPa–1 MPa range. These waves typically induce particle velocities (U_{p2}) on the order of 10–300 m/s, and can be produced by air blasts in the mid-to-far-field. Soldiers in Iraq and Afghanistan often encounter shock waves of this magnitude, which can result in mild to severe traumatic brain injury (TBI), and long-term medical problems [1]. Thus, many recent experimental [2–4] and computational [5,6] works have centered around the response of polymer and polymer-composites to these types of threats.

* Corresponding author. Tel.: +1 8452421687.
E-mail address: frs122@psu.edu (F.R. Svingala).

0734-743X/$ – see front matter © 2012 Elsevier Ltd. All rights reserved.
http://dx.doi.org/10.1016/j.ijimpeng.2012.08.006

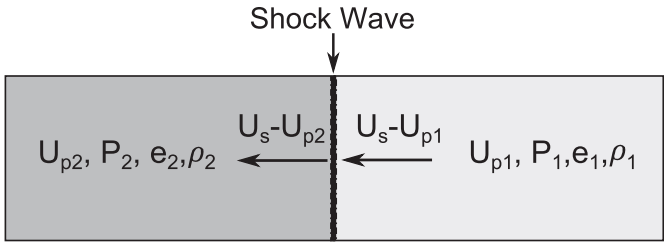

Fig. 1. Reference diagram for steady Rankine–Hugoniot equations. Coordinate frame is fixed to the shock wave and material moves from right to left.

However, shock Hugoniot data for polymers that are available in the literature are typically confined to shock waves inducing particle (U_{P2}) velocities greater than 500 m/s [7]. Simple materials, such as common metals, generally exhibit a linear U_s–U_{p2} relationship, allowing high-velocity data to be simply extrapolated to lower particle velocities. More-complex materials, however, may undergo a primary or secondary phase transition in this region, altering the shape of the U_s–U_{p2} curve and making a blind extrapolation misleading and inaccurate. Measurements of the polymethyl methacrylate (PMMA) shock Hugoniot, for example, reveals a significant downward curvature below a particle velocity of $U_{p2} \cong 300$ m/s [8]. Porter and Gould suggest that this more-complex behavior in polymers is due to a combination of the collapse of ring groups and the long molecular relaxation times associated with high-molecular-weight polymers [9]. To accurately predict the shock response of polymers and other complex materials in this region it is therefore important to rely on experimental data rather than extrapolations of higher-velocity shock Hugoniot data.

Experimentally defining a shock Hugoniot requires the initiation of a shock wave in the material of interest, and simultaneous measurement of any two variables in the shocked state, i.e., U_{p2}, P_2, U_s, e_2, or ρ_2. In practice, U_{p2}, P_2, and U_s are the most readily observed. These measurements must be made in the region of 1-D strain immediately behind the shock wave in order to satisfy equations (1), (2), and (3).

There are many methods of initiating a shock wave in the laboratory, the most common being a ballistic projectile accelerated up to as much as several km/s by a light gas gun [10]. U_s and U_{p2} may be measured by laser interferometry at the back surface of the sample or P_2 may be measured with single-use manganin gages [11,12]. Each of these tests produces a constant-strength shock, allowing a single point of the shock Hugoniot curve to be measured. Determining the entire shock Hugoniot in this manner thus requires an extensive series of impact experiments.

In the present work, optical methods for determining the shock Hugoniot of transparent and opaque materials are explored. The passage of a shock wave changes the local material density, which results in a change in the local index of refraction [13]. If the material of interest has at least some transparency, the refractive index field within the material can be visualized by the schlieren or shadowgraph technique [13]. The shadowgraph technique was previously explored by Yamada et al., who measured the shock Hugoniot for PMMA optically, using shadowgraphy and a high-speed-film streak camera in 1978 [14]. This previous work observed a single shock velocity and inferred the particle velocity from the motion of the back surface of the sample.

The present work further develops this technique in two main ways: optical measurement of the shock Hugoniot is extended to opaque materials, even those which exhibit spallation or void formation that alters motion of the sample's free-surface, and the measurement of multiple points of the shock Hugoniot of transparent materials in a single experiment with an explosively-driven shock wave. Using these techniques, the shock Hugoniot of two polymers of interest for ballistic and blast protection (a polyurethane and a polyurea) are experimentally extended for shocks inducing $U_{p2} < 250$ m/s.

2. Experimental methods

2.1. Apparatus and materials

The stress and shock wave properties of two polymers are investigated here: a clear polyurethane (Ultralloy Ultraclear 435) and a semi-opaque polyurea (Air Products Versalink P1000 combined with Dow Chemical Isonate 143L at a 4:1 ratio). Stress waves are also examined in a polycarbonate bar obtained from McMaster-Carr.

Wave motion was visualized by a 100 mm diameter, f/9.6, lens-type shadowgraph system with a Photron SA-5 high-speed-digital camera recording at up to 10^6 frames/s (Fig. 2). Shadowgraph illumination was provided by a 200 W Hg-Xenon arc lamp. A principal advantage of this system is the lack of complicated triggering requirements; typical high-speed optical methods used in shock physics often require the use of an argon flash, streak camera or both [15]. Both require very precise triggering with respect to the shock event and each other in order to successfully observe the event of interest. By using a continuous arc lamp and a high-speed digital camera with a recording time on the order of 5 s, triggering problems are eliminated, making this experimental apparatus much less difficult to set up and use.

2.2. Stress wave visualization and sound speed measurement

Shadowgraph stress wave tracking was performed on 25 mm × 25 mm × 25–60 mm rectangular bars of transparent polyurethane and polycarbonate and semi-opaque polyurea. Stress waves were initiated by the explosion of 0.4 mm diameter copper exploding bridge-wires (EBW) by a 125 J capacitor discharge.

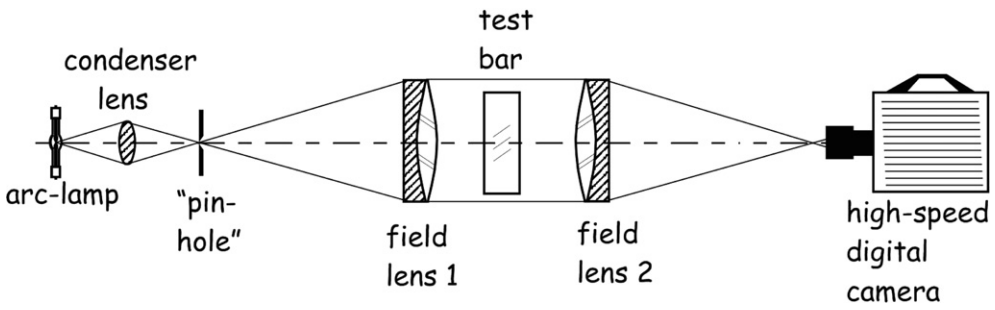

Fig. 2. A schematic diagram of the shadowgraph system used in this investigation.

Stress waves are relatively-weak disturbances and, as such, are not easily visible in the raw shadowgraph images. To increase the visibility of these waves, a digital background subtraction procedure was performed on each image. A pre-test 'tare' image was subtracted from each subsequent image, so that changes from the initial, wave-free state were highlighted. Fig. 3 demonstrates the results of this process. The speed of the stress wave could then be measured by tracking the position of the wavefront in the high-speed shadowgraph record. Ultrasonic sound speed measurements were also performed on these polymers. Measurements of both the longitudinal (c_l) and shear (c_s) sound speeds were performed with 5 MHz transducers in a pitch-catch arrangement.

2.3. Constant-velocity shock wave Hugoniot measurement

Constant-velocity shock waves were generated in both polyurethane and polyurea sample plates by ballistic impact. Samples with a 25 × 25 mm cross-section were struck by 25 mm diameter 2024-Al cylinders accelerated to velocities of 90–250 m/s by a light gas gun (Fig. 4). Projectile and sample lengths were chosen to ensure a steady, 1-D shock wave throughout the experiment [10]. This wave initially sets up a 1-D strain condition in the sample, but lateral relief at the sides of the sample (Fig. 5) lead to the production of an expansion wavefront traveling at the local longitudinal sound speed [16]. Passage of this expansion wavefront relieves the state of 1-D strain, and begins a transition to a state of 1-D stress. All present Hugoniot measurements are made on centerline in the period of 1-D strain before this relief reaches the central axis, about 5 μs and 7 μs after the shock passes.

Shock velocity was measured in semi-opaque samples by dividing the optically-measured shock transit time by sample length, and in transparent samples by tracking the position of the shock front in each frame of the high-speed shadowgraph record. Particle velocities were measured by tracking the motion of the projectile/polymer-sample interface after impact and by free-surface tracking. In ballistic testing of polyurea, an auxiliary halogen lamp was used to illuminate the reflective aluminum projectile in order to make the projectile-sample interface more visible.

Due to the reflection of a release wave from the free-surface, free-surface velocity is not directly equal to U_{p2}. To calculate U_{p2} the free-surface approximation [15], equation (4), is applied using:

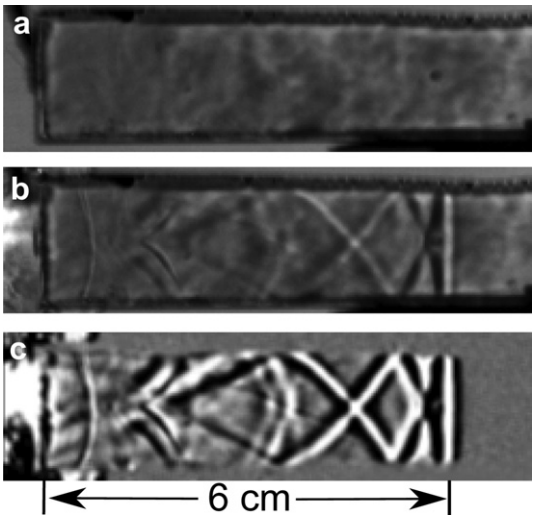

Fig. 3. Polycarbonate bar, a) pretest, b) raw shadowgram of stress wave, c) same image after processing, wave motion is from left to right.

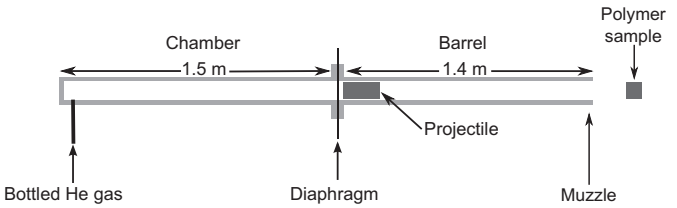

Fig. 4. A schematic diagram of the light gas gun used in this investigation.

$$U_{p2} = \frac{U_{fs}}{2} \tag{4}$$

where U_{fs} is the measured free-surface velocity. This assumption is nearly exact for the relatively-low shock pressures used in this work, and is discussed in detail elsewhere [17]. Each ballistic impact experiment allows the measurement of a single U_s–U_{p2} combination, defining a single point of the shock Hugoniot.

2.4. Decelerating shock wave Hugoniot measurement

Decelerating shock waves were next induced in rectangular polyurethane samples by detonating one to 2 g of pentaerythritol tetranitrate (PETN), a high-explosive. A 13 mm diameter cylindrical hole was drilled into each polymer sample to the depth required to accommodate the desired amount of powdered PETN at a packing density of 1 ± 0.05 g/cc. This cylinder was filled with PETN and capped with a PETN hemisphere as shown in Fig. 6. The charge was initiated by an EBW placed between the hemisphere and cylinder (for the details of this initiation method, see ref [18]). The bridgewire and PETN hemisphere were held in place by a few drops of nitrocellulose thinned with acetone to form an "explosive adhesive". The gram-scale explosive charge produces an initially-high pressure and a strong shock wave by direct coupling of the detonation wave into the polymer sample. As the unconfined gaseous explosive products expand after detonation, pressure at the sample surface is quickly reduced. This generates a continuous series of release waves within the sample which, in concert with the effects of viscoelasticity, slow the shock wave as it transits the long rectangular samples used in these experiments. If the sample is transparent, multiple shock- and particle–velocity combinations may be observed in a single experiment.

Shock velocities were measured by tracking the position of the shock front in the high-speed shadowgraph record. Particle velocities were observed by free-surface tracking, as was done in the constant-velocity shock testing, and by tracking the position of internal fiducials. These fiducials were small (diameter ≤0.1 mm)

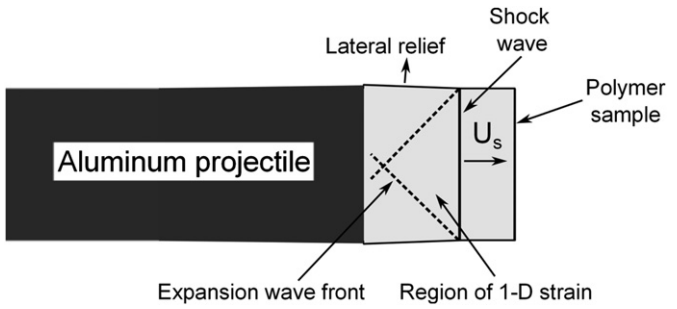

Fig. 5. Diagram of the lateral relief process after passage of a shock wave. The aluminum projectile moves from left to right. The shock wave in the polymer sample is represented by a solid line, and the first expansion wave from each surface is represented by a dashed line. All Hugoniot measurements in the present work are made in the triangular region of 1-D strain before the arrival of the expansion wavefront.

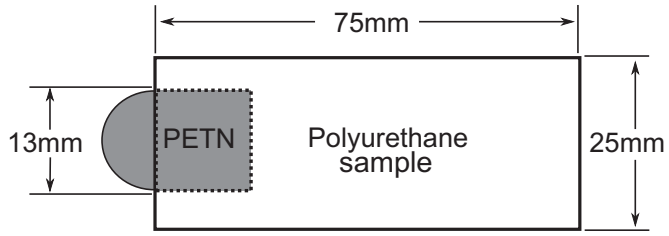

Fig. 6. PETN charge arrangement used to induce shock waves in rectangular polyurethane samples.

air inclusions introduced during the polymer sample plate molding process. As these fiducials were observed through a deformed surface (see Fig. 5) they were subject to a lens effect, which altered their observed positions. The shape of the optical surfaces of the polymer sample plates used here were observed to be a wedge of constant slope for an interval of 8–10 μs after the passage of the shock wave. This wedge shape shifts the observed position of all of the internal fiducials by a constant value, and thus has no effect on the measured particle velocities in this work. In general, the surface shape should be checked when applying this technique to other materials as there is no guarantee that all materials will exhibit this wedge-type surface shape.

3. Results and discussion

3.1. Stress wave imaging

These techniques were initially qualified with EBW-induced stress waves. The EBW applies a relatively small point impulse to the sample bar, producing a weak compression wave with $U_{p2} \cong 0$. The application of a point load produces an initially-spherical wavefront, which becomes completely flat after traveling about 4 times the width of the sample bar (Fig. 7). This change in shape is the result of a dynamic Saint-Venant effect, similar to those observed by Flynn and Frocht in transparent Bakelite bars [19].

These stress waves travel at the longitudinal sound speed in the material [20]. Stress wave speeds were observed in polycarbonate, polyurethane, and polyurea and were compared with ultrasonically-measured c_l values. In all cases, the wave speeds

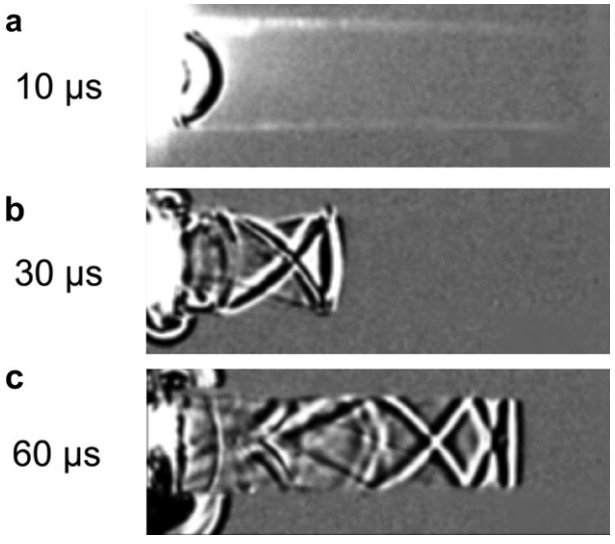

Fig. 7. Stress wave motion in polycarbonate demonstrating the development of a 1-D planar stress wave from an initial point load. Wave motion is from left to right, and times given are elapsed time after EBW detonation.

Table 1
Longitudinal sound speeds as observed by ultrasound and shadowgraph techniques, all values in m/s.

	Ultrasound c_l m/s	Shadowgraph c_l m/s
Polycarbonate	2189 ± 12	2160 ± 13
Polyurethane	2355 ± 16	2352 ± 3
Polyurea	1699 ± 15	1687 ± 4

measured by shadowgraph wave tracking were found to agree within the measurement error of those obtained by ultrasonic measurements (Table 1). This serves to validate the present optical approach by comparison.

3.2. Shock wave imaging and the shock Hugoniot

3.2.1. Constant-velocity shock waves

After each ballistic-impact experiment a pseudo-streak diagram, also known as a x-t diagram, was generated by cropping the same few rows of pixels from each frame of the high-speed shadowgraph record and assembling these vertically in order (Fig. 8(a)). This allows the entire time history of the wave propagation along the polymer sample to be displayed in a single diagram. In this plot, slope represents the inverse of velocity: zero velocity corresponds to a vertical line, with velocity increasing as slope approaches the horizontal.

An example pseudo-streak diagram of a ballistic impact experiment on polyurethane is shown in Fig. 8(b). The ballistic projectile enters from the left and strikes the transparent polyurethane sample, producing the primary shock wave indicated by B. The projectile–sample interface is labeled as A. U_{fs} is measured in the

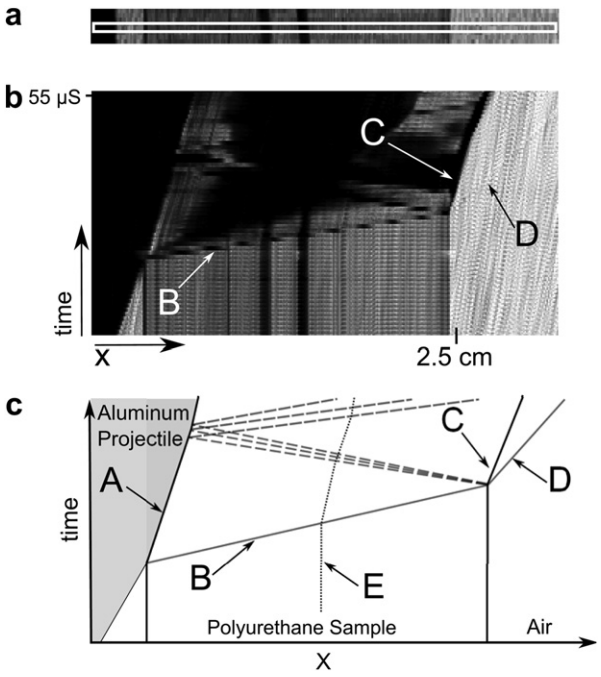

Fig. 8. (a): Raw frame from the high-speed shadowgraph record, with cropped area bounded in white. (b): Pseudo-streak diagram of a ballistic impact experiment in polyurethane, assembled from a temporal series of cropped images. The ballistic projectile enters from the left, striking the sample and producing a shock wave. The primary shock is labeled as B, U_{fs} is measured in the linear portion of the free-surface record, C. An air shock due to free-surface-motion is labeled as D. (c): Schematic wave diagram of the test shown in (b). Features are labeled as in (b), with the addition the projectile-sample interface, indicated by A, and a massless tracer particle, E. Solid lines represent shock waves, while dashed lines represent expansion waves.

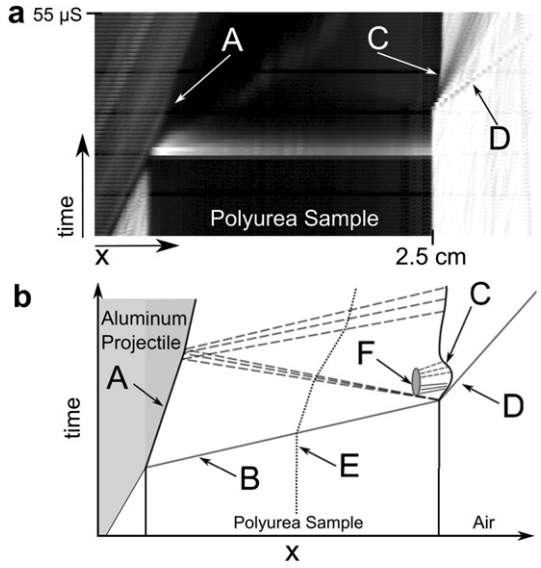

Fig. 9. (a): Shadowgraph streak diagram of ballistic impact test in a semi-opaque polyurea sample. Production of voids by the reflected rarefaction complicates motion of the free-surface, C. U_{p2} is, instead, measured at the projectile-sample interface, A, to avoid this phenomena. D indicates the shock wave transmitted through the sample into the air. (b): Schematic wave diagram of the test shown in (a). Features are labeled as in (a), with the addition of the primary shock, B, a massless tracer particle, E, and area of void formation/collapse, F. Solid lines represent shock waves, and dashed lines represent expansion waves.

linear portion of the free-surface record, C. U_s is obtained by tracking the position of the primary shock as a function of time. U_{p2} in polyurethane samples may be obtained by tracking the projectile–sample interface or through U_{fs} and equation (4).

Fig. 9(a) shows the pseudo-streak diagram for a polyurea sample. Since this sample is not transparent, internal features are not visible. Nevertheless, primary shock transit time can be measured by noting the time of impact and the appearance of the transmitted shock wave in air (indicated by D).

The free-surface velocity (C) in polyurea samples was observed to lack the significant linear portion observed in polyurethane tests, making accurate determination of U_{p2} from U_{fs} difficult. Microscopy of the polyurea samples after testing revealed the formation of voids or tears 4–5 mm from the free-surface of the sample, visible in Fig. 10. This effect was not observed in the polyurethane samples. It is likely that these voids are created by the interaction of release waves reflected from free-surfaces of the sample. The interaction of these waves produces a transient region of high tensile stress, leading to localized void nucleation [21]. The formation and collapse of these voids leads to the observed more complex motion of the free-surface as a function of time. This process and its interaction with the free-surface is shown schematically in Fig. 9(b), labeled as F.

These voids cannot have any influence on U_{fs} until pressure waves produced by their expansion reach the free-surface. An estimate of the travel time for a pressure wave from the area of void formation to the free-surface was made by assuming the pressure waves travel at c_l. This gives a result of 2.3 μs. At least two frames, or 2 μs, are required to perform a velocity measurement. Therefore, a valid U_{fs} may be recorded before material failure influences the result, however, due to the fact that the event time is very close to the temporal resolution of the camera, the error bar associated with this measurement is very high (±25 m/s). These polyurea experiments were then repeated with halogen front-lighting to reveal the projectile–sample interface. Since this interface is far from the voids, its velocity is unaffected by them for the duration of the test. Tracking the projectile–sample interface proved to be a more precise method of measuring U_{p2}, with error bars of 1–5 m/s.

3.2.2. Decelerating shock waves

Detonation of the high-explosive produces an initially high pressure, driving a strong shock into the sample. The peak pressure applied to the sample may be estimated *a priori* from the detonation parameters of the high-explosive used and the packing density of the charge. The peak pressure can be calculated by an impedance-match solution between the Hugoniots of the PETN reaction products and the polyurethane. The PETN explosive was packed to 1 g/cc, which resulted in a peak pressure in the polyurethane of 9.3 GPa [22]. By varying the packing density of PETN, this peak pressure could be varied from 4 to 30 GPa [22].

The rate at which the shock wave decelerates is controlled by the pressure-time profile at the interface between the explosive and sample, shown schematically in Fig. 11. This profile can be modified by changing the thickness of the high-explosive charge or the confinement of the gaseous products of detonation, or both. Thicker high-explosive charges produce greater quantities of product gas, which expand more slowly and thus produce a longer pressure pulse. Radial confinement of the explosive charge resists

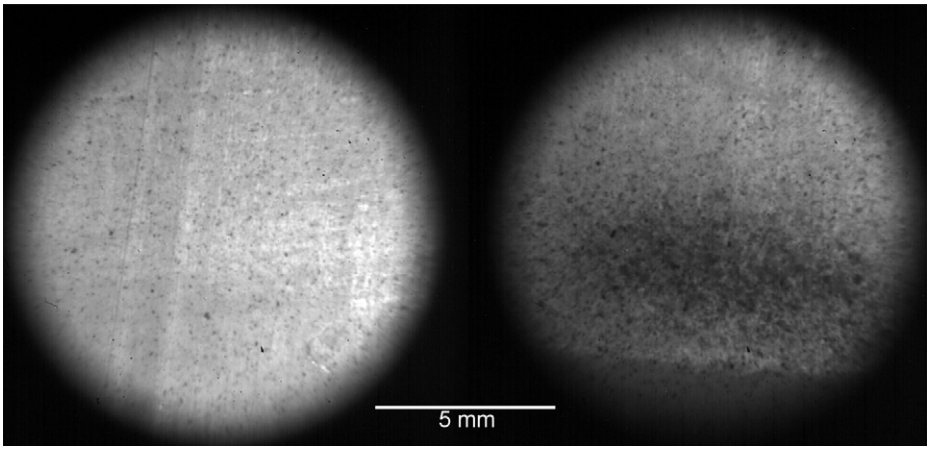

Fig. 10. Micrographs, left, untested polyurea with few visible voids; right, polyurea with voids formed by interaction of tensile waves after the shock wave reflects from the back surface of the sample.

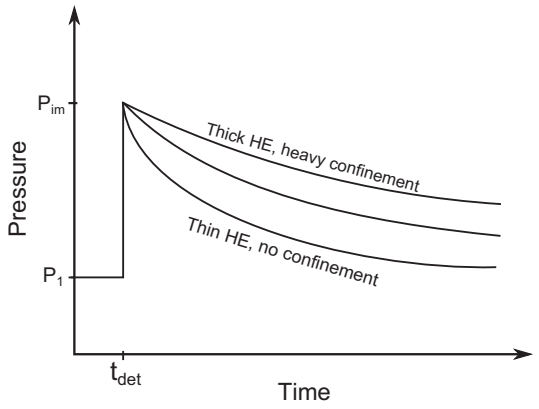

Fig. 11. Schematic pressure-time plot at the high-explosive-polymer interface [22]. P_1 is the unshocked pressure of the sample, P_{im} is the pressure calculated by impedance matching between the explosive products and the sample, and t_{det} the time of detonation.

the expansion of the product gases, also contributing to a longer pressure pulse [22]. In these experiments, confinement and high-explosive thickness were chosen to allow observation of the shock over the range $0 \leq U_{p2} \leq 250$ m/s.

Previous efforts utilizing high explosives to generate shock Hugoniot data have required orders of magnitude more explosive than the technique presented here [15,23]. In comparison the use of a 1–2 g lab-scale explosive charge has several advantages: the test may be more easily observed by delicate instruments, such as optics and high speed cameras, cost is greatly reduced by eliminating the need for a full-sized explosives range or bunker, and risk to the investigators involved is much reduced.

A pseudo-streak diagram of a high-explosive test is shown in Fig. 12. The white region, indicated by A, is the direct light generated by the detonation of the explosive. The primary shock wave, B, can be seen propagating from left to right. As it passes, fidcuials present in the sample, C, are accelerated from rest and act as U_{p2} tracers. The shock then reflects at the far side of the sample,

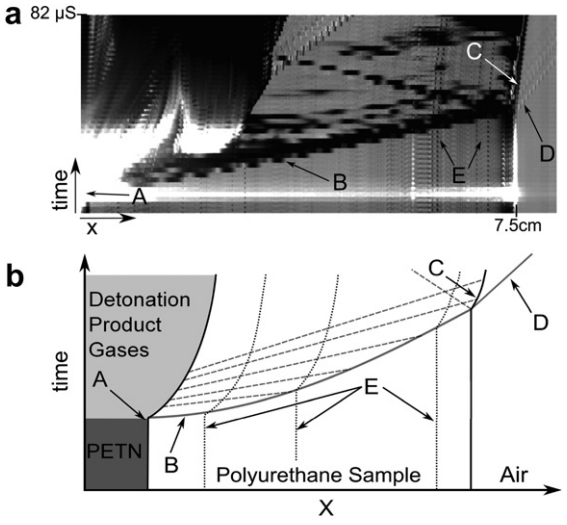

Fig. 12. (a): Shadowgraph pseudo-streak diagram of explosively-generated shock motion in polyurethane. A indicates direct light from the detonation of the explosive, B the primary shock wave, C the free-surface motion, D the transmitted air shock, and E, a few internal fiducials. (b): Schematic wave diagram of the test shown in (a), with primary shock curvature exaggerated for clarity. Solid lines represent shock waves and dashed lines represent expansion waves.

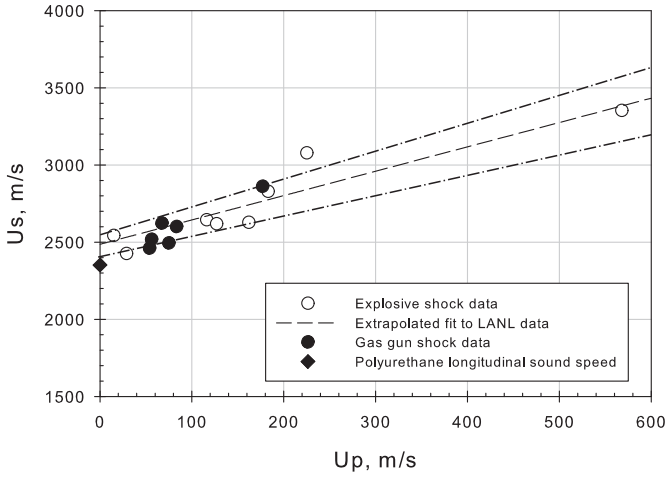

Fig. 13. Shock Hugoniot data for Polyurethane. Empty circles represent explosively-generated data, with associated error band represented by dot-dash lines. Filled circles represent ballistic projectile data. The dashed line represents an extrapolated fit from LANL gas-gun data [22].

setting the free-surface (E) into motion and providing another opportunity to measure U_{p2}. With optical access to the entire sample, the use of a decelerating shock wave allows multiple (U_s,U_{p2}) combinations to be observed in a single experiment. Each U_{p2} value is measured within 3–4 /mu s of the passage of the shock front.

3.2.3. Shock Hugoniot data

The shock Hugoniot data collected by the methods described above are shown on the U_s–U_{p2} plane for polyurethane and polyurea in Figs. 13 and 14, respectively. The explosively-generated shock Hugoniot for transparent polyurethane is in very good agreement with the ballistic projectile results. These results also agree with an extrapolation of a LANL shock Hugoniot for polyurethane, measured for $659 < U_{p2} < 5078$ m/s [24]. This indicates that polyurethane does not undergo any significant phase changes in the previously-unobserved region of $U_{p2} < 250$ m/s.

The significant error band of the decelerating shock results is shown to increase with increasing shock velocity (Fig. 13). This is

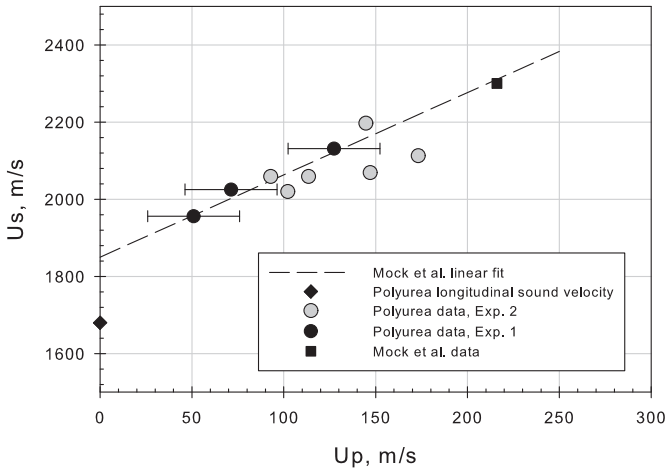

Fig. 14. Shock Hugoniot data for Polyurea. Black circles represent data from experiment 1, with no front lighting. Gray circle represent data from experiment 2, with front lighting to reduce the measurement error in U_{p2}. Data and a linear fit proposed by Mock et al. are shown for comparison [25].

due to temporal resolution limitations of the high-speed camera used in this investigation. As shock speed increases, the wavefront moves a greater distance between frames, increasing spatial averaging of the shock speed. To overcome this, a faster framing camera or a high-speed streak camera could be used to provide increased temporal resolution. Unfortunately, these resources were unavailable for this investigation.

The shock Hugoniot of the semi-opaque polyurea was also successfully measured (Fig. 14). Experiment set 1 was performed without front lighting, with U_{p2} calculated from the free-surface motion (Fig. 9). Experiment set 2 was performed with front lighting, with U_{p2} directly measured at the projectile–sample interface. These different approaches yield essentially-identical results. The measured Hugoniot was also found to be in substantial agreement with an extrapolation of an available Hugoniot for a similar polyurea, measured for $216 < U_{p2} < 793$ [25]. The explosively-generated decelerating shock method could not be applied to these samples (represented in Fig. 14) due to their poor transparency.

4. Conclusions

Modern digital high-speed camera technology was combined with the shadowgraph technique to measure the shock Hugoniot of a transparent polyurethane and a semi-opaque polyurea. Waves were generated by exploding-bridge-wires, aluminum ballistic projectiles, and gram-scale high-explosive charges. The constant-velocity shock wave induced by a ballistic projectile allows observation of a single (U_s, U_{p2}) point per test in both transparent and opaque materials. In transparent materials the shock wave may be observed throughout the sample plate; if the shock wave decelerates as it transits the sample, multiple U_s–U_{p2} points to be measured in a single test, reducing the number of tests required to fully define a shock Hugoniot. In this work, decelerating waves were produced by gram-scale high-explosive charges, but a similar decelerating wave could also be generated with a modified shock tube [26]. In all cases, Hugoniot data extrapolated from other investigations using stronger shock waves agree with data measured in this work, indicating that neither the polyurethane nor the polyurea examined here undergo a significant phase change in the region of $U_{p2} < 250$ m/s.

By using optical techniques and modern high-speed digital imaging, shock Hugoniot curves may be developed more readily than with traditional, non-optical point-by-point methodology. The approach presented in this work generates shock Hugoniot data with fewer experiments, without the use of costly consumables such as manganin pressure gages, and without cumbersome precision triggering. It also requires only an ordinary laboratory space, not an explosives range or bunker. As presented, this method is appropriate for measuring shock velocites below approximately 3.5 km/s, limited only by the temporal resolution of the camera used.

References

[1] Okie S. Traumatic brain injury in the war zone. New England Journal of Medicine 2005;352(20):2043–7.
[2] Gardner N, Wang E, Kumar P, Shukla A. Blast mitigation in a sandwich composite using graded core and polyurea interlayer. Experimental Mechanics 2012;52:119–33.
[3] Amini MR, Isaacs J, Nemat-Nasser S. Investigation of effect of polyurea on response of steel plates to impulsive loads in direct pressure-pulse experiments. Mechanics of Materials 2010;42(6):628–39.
[4] McShane G, Stewart C, Aronson M, Wadley H, Fleck N, Deshpande V. Dynamic rupture of polymer-metal bilayer plates. International Journal of Solids and Structures 2008;45(16):4407–26.
[5] Grujicic M, Pandurangan B, He T, Cheeseman B, Yen C, Randow C. Computational investigation of impact energy absorption capability of polyurea coatings via deformation-induced glass transition. Materials Science & Engineering: A (Structural Materials: Properties, Microstructure and Processing) 2010;527(29–30):7741–51.
[6] Grujicic M, Bell WC, Pandurangan B, He T. Blast-wave impact-mitigation capability of polyurea when used as helmet suspension-pad material. Materials and Design 2010;31:4050–65.
[7] Carter W, Marsh S. Hugoniot equation of state of polymers. Tech. Rep. LA-13006-MS. NM: Los Alamos National Lab.; 1995.
[8] Schmidt D, Evans M. Shock wave compression of 'plexiglas' in the 2.5 to 20 kilobar region. Nature 1965;206:1348.
[9] Porter D, Gould PJ. Predictive nonlinear constitutive relations in polymers through loss history. International Journal of Solids and Structures 2009; 46(9):1981–93.
[10] Jones AH, Isbell WM, Maiden CJ. Measurement of the very-high-pressure properties of materials using a light-gas gun. Journal of Applied Physics 1966;37(9):3493–9. http://dx.doi.org/10.1063/1.1708887.
[11] Barker RE, Hollenbach LM. Shock-wave studies of PMMA, fused silica, and sapphire. Journal of Applied Physics 1970;41:4208–26.
[12] Yiannakopoulos G. A review of manganin gauge technology for measurements in the gigapascal range. Tech. Rep. MRL-TR-90–5. Ascot Vale (Australia): Materials Research Labs; 1990.
[13] Settles GS. Schlieren and shadowgraph techniques. Berlin: Springer; 2001. p. 25–75.
[14] Yamada T, Kani K, Morita A. Shock compression of polymethylmethacrylate from 20 to 80 kilobars. In: Shin-Ichi Hyodo, editor. Proceedings of the 13th international congress on high speed photography and photonics. 1978. p. 743–6.
[15] Wackerle J. Shock-wave compression of quartz. Journal of Applied Physics 1962;33(3):922. http://dx.doi.org/10.1063/1.1777192.
[16] Radford D, Willmott G. Failure mechanisms in ductile and brittle materials during Taylor impact. Journal de Physique IV 2003;110:687–92.
[17] Walsh JM, Christian RH. Equation of state of metals from shock wave measurements. Physics Review 1955;97:1544–56. http://dx.doi.org/10.1103/PhysRev.97.1544.
[18] Hargather MJ, Settles GS. Optical measurement and scaling of blasts from gram-range explosive charges. Shock Waves 2007;17(4):215–23. http://dx.doi.org/10.1007/s00193-007-0108-8.
[19] Flynn P, Frocht M. Experimental mechanics 1 (January).
[20] Kinslow R, Cable A. High-velocity impact phenomena. Academic Press; 1970.
[21] Chapman DJ, Radford DD, Reynolds M, Church PD. Shock induced void nucleation during Taylor impact. International Journal of Fracture 2005;134:41–57.
[22] Cooper PW. Explosives engineering. Wiley-VCH; 1996.
[23] Katz S, Doran DG, Curran DR. Hugoniot equation of state of aluminum and steel from oblique shock measurement. Journal of Applied Physics 1959; 30(4):568–76. http://dx.doi.org/10.1063/1.1702407.
[24] Marsh S. LASL shock Hugoniot data. In: Los Alamos Scientific laboratory series on dynamic material properties, vol 5. University of California Press; 1980.
[25] Mock Jr W, Bartyczak S, Lee G, Fedderly J, Jordan K. Dynamic properties of polyurea 1000. AIP Conference Proceedings 2009;1195(1):1241–4.
[26] Medvedev S, Polenov A. Simulation of non-ideal explosions in a conical shock tube. In: Raymond Brun, Lucien Z. Dumitrescu, editors. Shock waves at Marseille IV: shock structure and kinematics, blast waves and detonations. Proceedings of the 19th international symposium on shock waves. Berlin: Springer; 1995. p. 381–6. Marseille, France.